Supporting Information for

Temperature Determines Zika, Dengue and Chikungunya Transmission Potential in the Americas

Erin A. Mordecai, Jeremy M. Cohen, Michelle V. Evans, Prithvi Gudapati, Leah R. Johnson, Kerri Miazgowicz, Courtney C. Murdock, Jason R. Rohr, Sadie J. Ryan, Van Savage, Marta Shocket, Anna Stewart Ibarra, Matthew B. Thomas, Daniel P. Weikel
correspondence to: emordeca@stanford.edu

This PDF file includes:

Supplementary Results

Validation analyses with human incidence versus temperature datasets

We constructed a linear mixed effects model of the maximum relative incidence for the PAHO DENV, CHIKV, and ZIKV datasets as a function of virus species, log of percent of GDP in tourism, predicted R_0 from the mechanistic model, and the interaction of the latter two, with country as a random effect. The main effect of virus species was not a statistically significant predictor of observed incidence, indicating that the virus species did not differ in their observed outbreak sizes. Predicted R_0 from the mechanistic model ($X^2 = 10.26$, $df = 1$, $p = 0.001$) and its interaction with the log of percent of GDP in tourism ($X^2 = 4.14$, $df = 1$, $p = 0.042$) significantly predicted the observed maximum relative incidence (Fig. 2; results held when we dropped the ZIKV data, which were mostly from Colombia). When the percent of GDP in tourism is low, efforts to minimize human contacts with mosquitoes might also be low and the model based on temperature suitability alone is indeed predictive of the maximum size of observed epidemics (left and center panels in Fig. 2). When the percent of GDP in tourism is high, efforts to minimize human contacts with mosquitoes are also presumably high and thus the model based on temperature suitability alone is not very predictive of maximum epidemic size (right panel in Fig. 2). This is when the model based on temperature alone has a high false positive rate.

Sensitivity analyses

Because no temperature-sensitive vector competence or extrinsic incubation period (EIP) data were available for CHIKV or ZIKV, we were particularly interested in the R_0 model sensitivity to the thermal responses for these traits. We explored the impact of changes in *b, c,* and *PDR* by calculating R_0 for all posterior parameter samples with those focal traits shifted in the following ways: entire curves shifted ±3°C and ±5°C for all three traits, entire curves shifted ±3°C and ±5°C for each trait individually, and curves made 3°C wider or narrower without changing the mean for all three traits. We examined the impact of each modification on the thermal minimum, maximum, and optimum (T_0, T_m, and T_{pk}) for R_0. For *Ae. albopictus*, all shifts in trait thermal responses shifted T_{pk} by < 1°C, T_0 by approximately the amount of the trait shift (e.g., +3°C for the models with the traits shifted by +3°C), and had little effect on T_m (Fig. S11). Similarly, for *Ae. aegypti* all models shifted T_{pk} by < 2°C, T_0 by less than or equal to the amount of the trait shift, and had little effect on T_m, with the exception of the -5°C trait shift, which reduced T_m by 5°C (Fig. S12). These analyses indicate that the optimal and maximum temperatures for transmission are robust to error in the vector competence and EIP thermal responses. By contrast, the minimum and maximum temperature for transmission may be sensitive to these trait thermal responses, so it is important to experimentally measure vector competence and EIP, particularly at low temperatures, for each mosquito and pathogen species pair of interest.

We also used sensitivity analyses to characterize the degree to which the temperature response of each individual trait drives the overall temperature response of R_0 (i.e., $(1/R_0)(dR_0/dX)$ for each parameter X). For both the *Ae. aegypti* and the *Ae. albopictus* models, we found that the *PDR* thermal response dramatically increased the response of R_0 to temperature (Figs. S13-S14). The *Ae. albopictus* model was additionally sensitive to the thermal response of adult mosquito lifespan, which had a negative effect on the sensitivity of R_0 to temperature (Fig. S13).

We were interested in which trait's thermal response was driving the difference in optimal temperature for *Ae. aegypti* versus *Ae. albopictus* transmission. To investigate this, we sequentially swapped thermal responses from one model to the other (e.g., calculated R_0 with all *Ae. albopictus* trait thermal responses except one from *Ae. aegypti* and vice versa). Mosquito lifespan was the key driver in the difference between the two R_0-versus-temperature models. Although the optimal temperatures for mosquito lifespan were similar, the thermal breadth was much narrower for *Ae. albopictus* than for *Ae. aegypti*. R_0 is strongly limited by short mosquito lifespans at high temperatures, where viral extrinsic incubation is very rapid, so expanding the thermal breadth for this trait has a large effect on the optimum.

Uncertainty analyses

We estimated how uncertainty in the trait thermal responses contributed to uncertainty in R_0 versus temperature. First, we calculated the width of the 95% credible interval for R_0 with all parameters sampled from their posterior distributions across temperatures. Then, we calculated the width of the 95% credible interval for R_0 when each trait was sampled from its posterior distribution individually, while the remaining parameters were fixed at their posterior mean. We compared the width of the intervals when just one parameter was sampled from its posterior distribution to the width when all parameters were sampled to calculate the relative contribution of each parameter to uncertainty at each temperature. For *Ae. albopictus*, mosquito lifespan (*lf*) contributed most to uncertainty from 24-35°C and transmission probability (*b*), followed by infection probability (*c*), contributed most to uncertainty from 16-24°C (Fig. S15). For *Ae. aegypti*, biting rate (*a*) contributed most to uncertainty from 29-35°C, transmission probability (*b*) contributed most to uncertainty from 13-28°C, and mosquito lifespan (*lf*), fecundity (*EFD*), and infection probability (*c*) all contributed substantially to uncertainty from 13-35°C (Fig. S16).

References

1. Wesolowski A, et al. (2015) Impact of human mobility on the emergence of dengue epidemics in Pakistan. *Proc Natl Acad Sci*:201504964.

2. Morin CW, Monaghan AJ, Hayden MH, Barrera R, Ernst K (2015) Meteorologically driven simulations of dengue epidemics in San Juan, PR. *PLoS Negl Trop Dis* 9(8):e0004002.

3. Liu-Helmersson J, Stenlund H, Wilder-Smith A, Rocklöv J (2014) Vectorial Capacity of Aedes aegypti: Effects of Temperature and Implications for Global Dengue Epidemic Potential. *PLoS ONE* 9(3):e89783.

4. Johansson MA, Powers AM, Pesik N, Cohen NJ, Staples JE (2014) Nowcasting the spread of chikungunya virus in the Americas. *PLoS ONE* 9(8):e104915.

5. Delatte H, Gimonneau G, Triboire A, Fontenille D (2009) Influence of temperature on immature development, survival, longevity, fecundity, and gonotrophic cycles of Aedes albopictus, vector of chikungunya and dengue in the Indian Ocean. *J Med Entomol* 46(1):33–41.

6. Ezeakacha N (2015) Environmental impacts and carry-over effects in complex life cycles: the role of different life history stages. *Dissertation*. Available at: http://aquila.usm.edu/dissertations/190.

7. Westbrook CJ (2010) Larval ecology and adult vector competence of invasive mosquitoes Aedes albopictus and Aedes aegypti for Chikungunya virus. Dissertation (University of Florida). Available at: http://etd.fcla.edu/UF/UFE0041830/westbrook_c.pdf [Accessed October 23, 2013].

8. Wiwatanaratanabutr S, Kittayapong P (2006) Effects of temephos and temperature on Wolbachia load and life history traits of Aedes albopictus. *Med Vet Entomol* 20(3):300–307.

9. Teng H-J, Apperson CS (2000) Development and Survival of Immature Aedes albopictus and Aedes triseriatus (Diptera: Culicidae) in the Laboratory: Effects of Density, Food, and Competition on Response to Temperature. *J Med Entomol* 37(1):40–52.

10. Muturi EJ, Lampman R, Costanzo K, Alto BW (2011) Effect of temperature and insecticide stress on life-history traits of Culex restuans and Aedes albopictus (Diptera: Culicidae). *J Med Entomol* 48(2):243–250.

11. Alto BW, Juliano SA (2001) Temperature effects on the dynamics of Aedes albopictus (Diptera: Culicidae) populations in the laboratory. *J Med Entomol* 38(4):548–556.

12. Westbrook CJ, Reiskind MH, Pesko KN, Greene KE, Lounibos LP (2010) Larval environmental temperature and the susceptibility of Aedes albopictus Skuse (Diptera: Culicidae) to chikungunya virus. *Vector-Borne Zoonotic Dis* 10(3):241–247.

13. Briegel H, Timmermann SE (2001) Aedes albopictus (Diptera: Culicidae): Physiological aspects of development and reproduction. *J Med Entomol* 38(4):566–571.

14. Calado DC, Silva MAN da (2002) Avaliação da influência da temperatura sobre o desenvolvimento de Aedes albopictus. *Rev Saúde Pública* 36(2):173–179.

15. Calado DC, Navarro-Silva MA (2002) Influência da temperatura sobre a longevidade, fecundidade e atividade hematofágica de Aedes (Stegomyia) albopictus Skuse, 1894 (Diptera, Culicidae) sob condições de laboratório. *Rev Bras Entomol* 46(1):93–98.

16. Xiao F-Z, et al. (2014) The effect of temperature on the extrinsic incubation period and infection rate of dengue virus serotype 2 infection in Aedes albopictus. *Arch Virol* 159(11):3053–3057.

17. Focks DA, Haile DG, Daniels E, Mount GA (1993) Dynamic life table model for Aedes aegypti (Diptera: Culicidae): analysis of the literature and model development. *J Med Entomol* 30(6):1003–1017.

18. Yang HM, Macoris MLG, Galvani KC, Andrighetti MTM, Wanderley DMV (2009) Assessing the effects of temperature on the population of Aedes aegypti, the vector of dengue. *Epidemiol Infect* 137(8):1188–1202.

19. Beserra EB, Fernandes CRM, Silva SA de O, Silva LA da, Santos JW dos (2009) Efeitos da temperatura no ciclo de vida, exigências térmicas e estimativas do número de gerações anuais de Aedes aegypti (Diptera, Culicidae). *Iheringia Sér Zool*. Available at: http://agris.fao.org/agris-search/search.do?recordID=XS2010500501 [Accessed September 10, 2015].

20. Rueda L, Patel K, Axtell R, Stinner R (1990) Temperature-dependent development and survival rates of Culex quinquefasciatus and Aedes aegypti (Diptera: Culicidae). *J Med Entomol* 27(5):892–898.

21. Tun-Lin W, Burkot T, Kay B (2000) Effects of temperature and larval diet on development rates and survival of the dengue vector Aedes aegypti in north Queensland, Australia. *Med Vet Entomol* 14(1):31–37.

22. Kamimura K, et al. (2002) Effect of temperature on the development of Aedes aegypti and Aedes albopictus. *Med Entomol Zool* 53(1):53–58.

23. Eisen L, et al. (2014) The impact of temperature on the bionomics of Aedes (Stegomyia) aegypti, with special reference to the cool geographic range margins. *J Med Entomol* 51(3):496–516.

24. Couret J, Dotson E, Benedict MQ (2014) Temperature, Larval Diet, and Density Effects on Development Rate and Survival of Aedes aegypti (Diptera: Culicidae). *PLoS ONE* 9(2):e87468.

25. Watts DM, Burke DS, Harrison BA, Whitmire RE, Nisalak A (1987) Effect of temperature on the vector efficiency of Aedes aegypti for dengue 2 virus. *Am J Trop Med Hyg* 36(1):143–152.

26. Alto BW, Bettinardi D (2013) Temperature and dengue virus infection in mosquitoes: independent effects on the immature and adult stages. *Am J Trop Med Hyg* 88(3):497–505.

27. Carrington LB, Armijos MV, Lambrechts L, Scott TW (2013) Fluctuations at a low mean temperature accelerate dengue virus transmission by Aedes aegypti. *PLoS Negl Trop Dis* 7(4):e2190.

28. Davis NC (1932) The effect of various temperatures in modifying the extrinsic incubation period of the yellow fever virus in Aedes aegypti. *Am J Epidemiol* 16(1):163–176.

29. Focks DA, Daniels E, Haile DG, Keesling JE (1995) A simulation model of the epidemiology of urban dengue fever: literature analysis, model development, preliminary validation, and samples of simulation results. *Am J Trop Med Hyg* 53(5):489–506.

30. McLean DM, et al. (1974) Vector capability of Aedes aegypti mosquitoes for California encephalitis and dengue viruses at various temperatures. *Can J Microbiol* 20(2):255–262.

31. McLean DM, Miller MA, Grass PN (1975) Dengue virus transmission by mosquitoes incubated at low temperatures. *Mosq News*. Available at: http://agris.fao.org/agris-search/search.do?recordID=US19760088008 [Accessed August 26, 2015].

32. Joshi DS (1996) Effect of fluctuating and constant temperatures on development, adult longevity and fecundity in the mosquito Aedes krombeini. *J Therm Biol* 21(3):151–154.

33. JALIL M (1972) Effect of temperature on larval growth of Aedes triseriatus. *J Econ Entomol* 65(2):625–626.

34. Lambrechts L, et al. (2011) Impact of daily temperature fluctuations on dengue virus transmission by Aedes aegypti. *Proc Natl Acad Sci* 108(18):7460–7465.

35. Reisen WK, Fang Y, Martinez VM (2006) Effects of temperature on the transmission of West Nile virus by Culex tarsalis (Diptera: Culicidae). *J Med Entomol* 43(2):309–317.

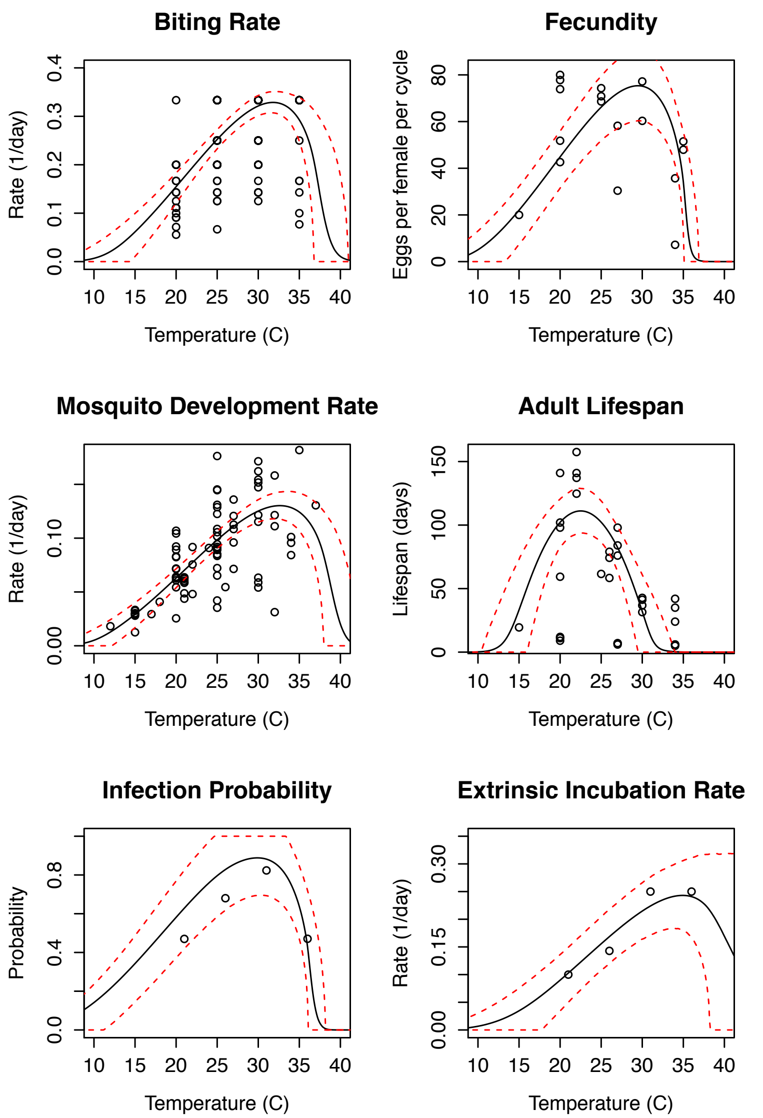

Fig. S1

Thermal responses of *Ae. albopictus* and DENV traits that drive transmission (parameter names and data sources listed in Table S1). Informative priors based on data from additional *Aedes* spp. and flavivirus studies helped to constrain uncertainty in the model fits (see Materials and Methods; Table S3). Points are the data. Black solid lines are the mean model fits; red dashed lines are the 95% credible intervals.

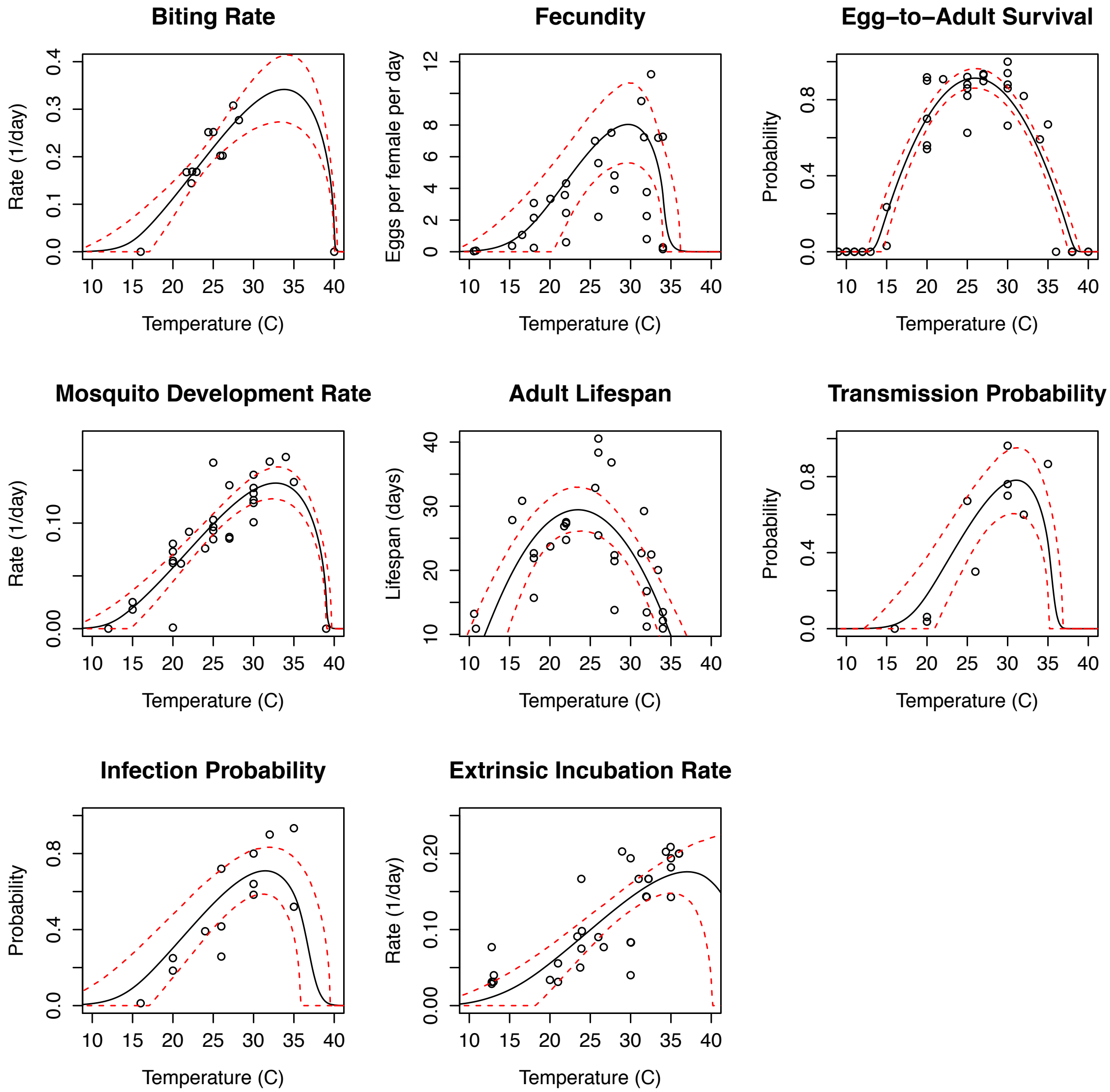

Fig. S2

Thermal responses of *Ae. aegypti* and DENV traits that drive transmission (parameter names and data sources listed in Table S2). Informative priors based on data from additional *Aedes* spp. and flavivirus studies helped to constrain uncertainty in the model fits (see Materials and Methods; Table S3). Points are the data. Black solid lines are the mean model fits; red dashed lines are the 95% credible intervals.

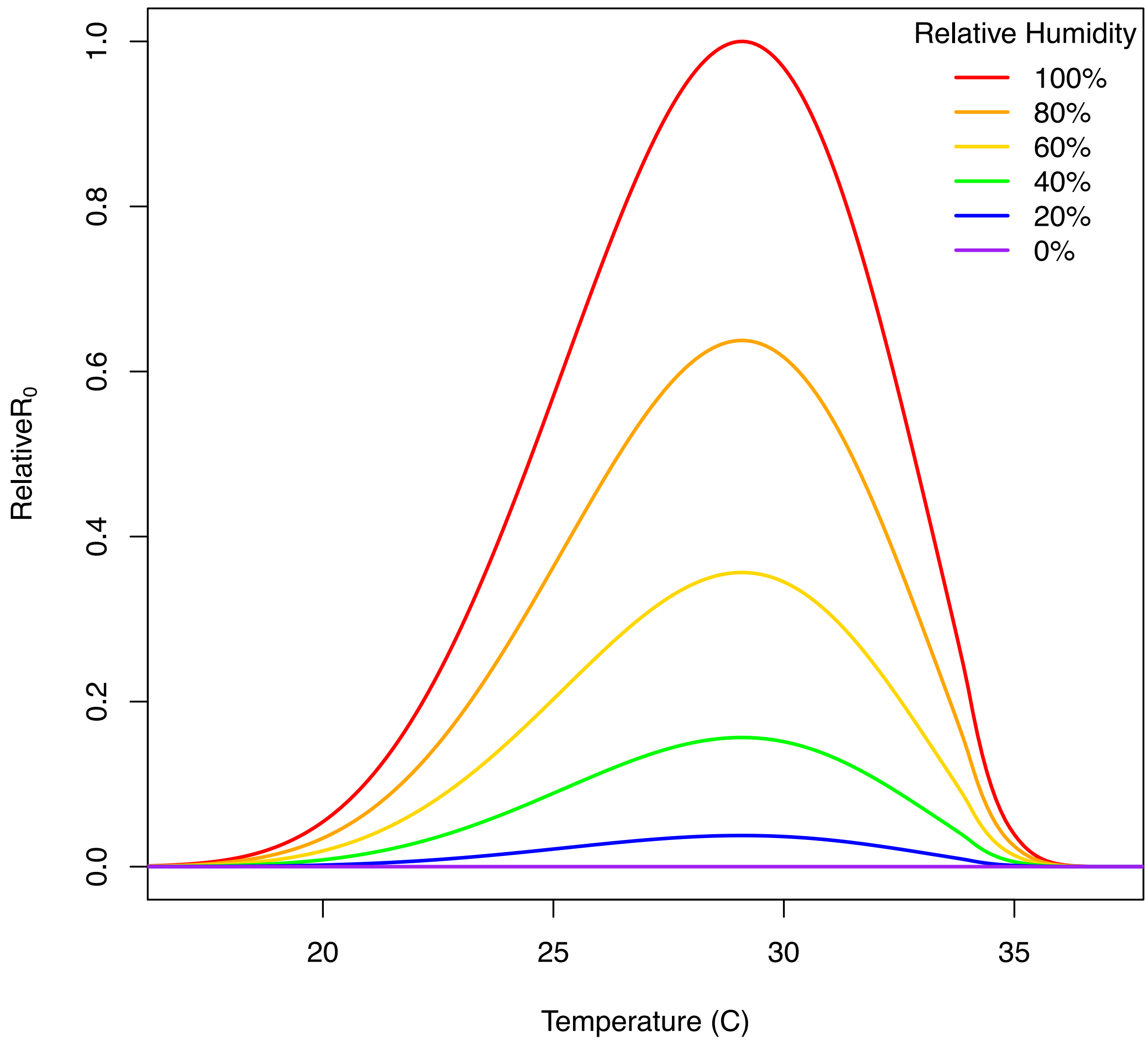

Fig. S3

Effects of relative humidity on relative R_0 versus temperature for *Ae. aegypti*, assuming constant temperatures. Humidity increases R_0 exponentially but does not affect the shape of the thermal response of R_0 (i.e., minimum, maximum, or peak temperature).

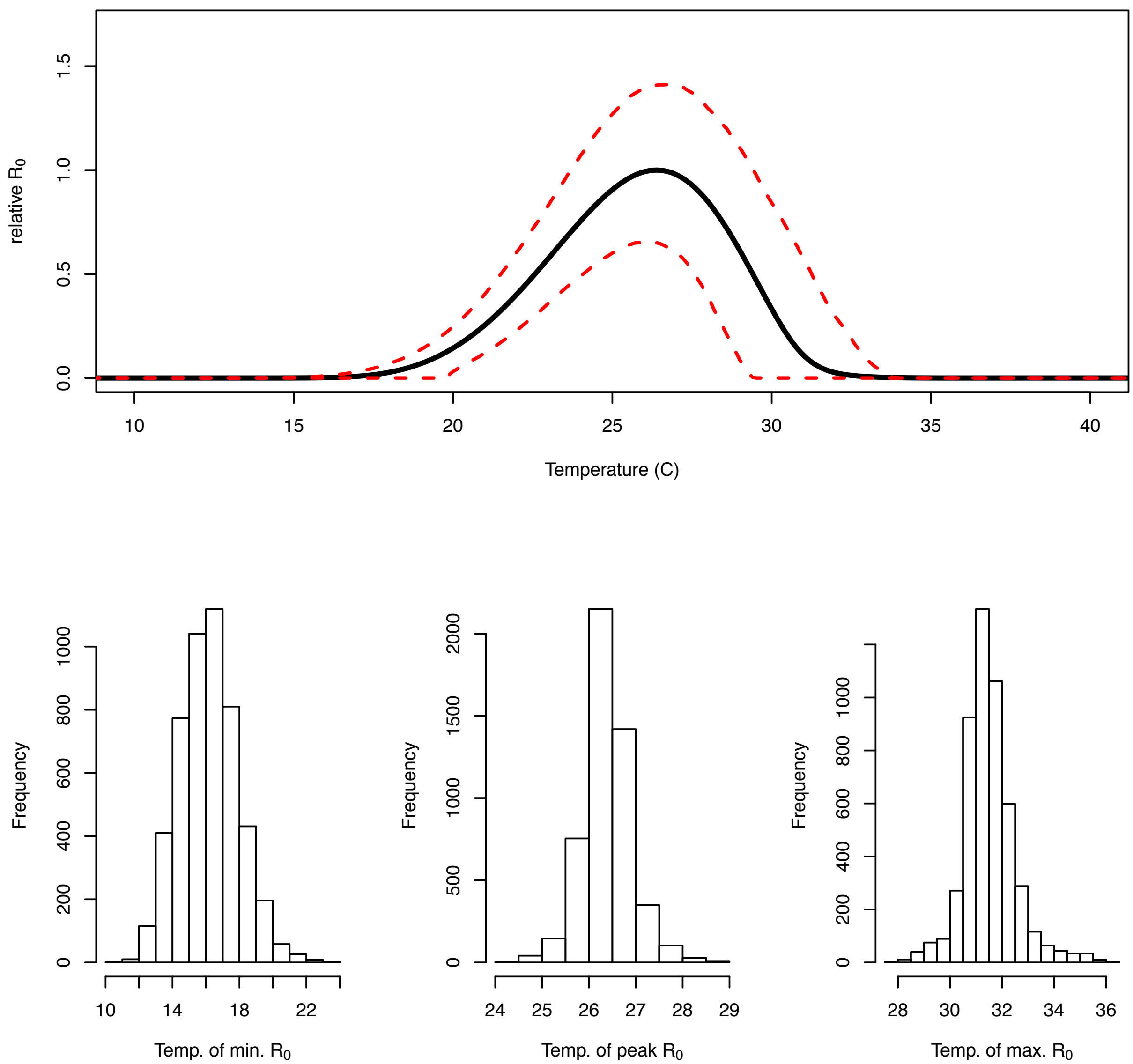

Fig. S4

Top, *Ae. albopictus* R_0 versus temperature, mean (black line) and 95% highest posterior density intervals (red dashed lines), for constant temperatures. Bottom, histograms of the minimum, maximum, and optimum temperatures for transmission.

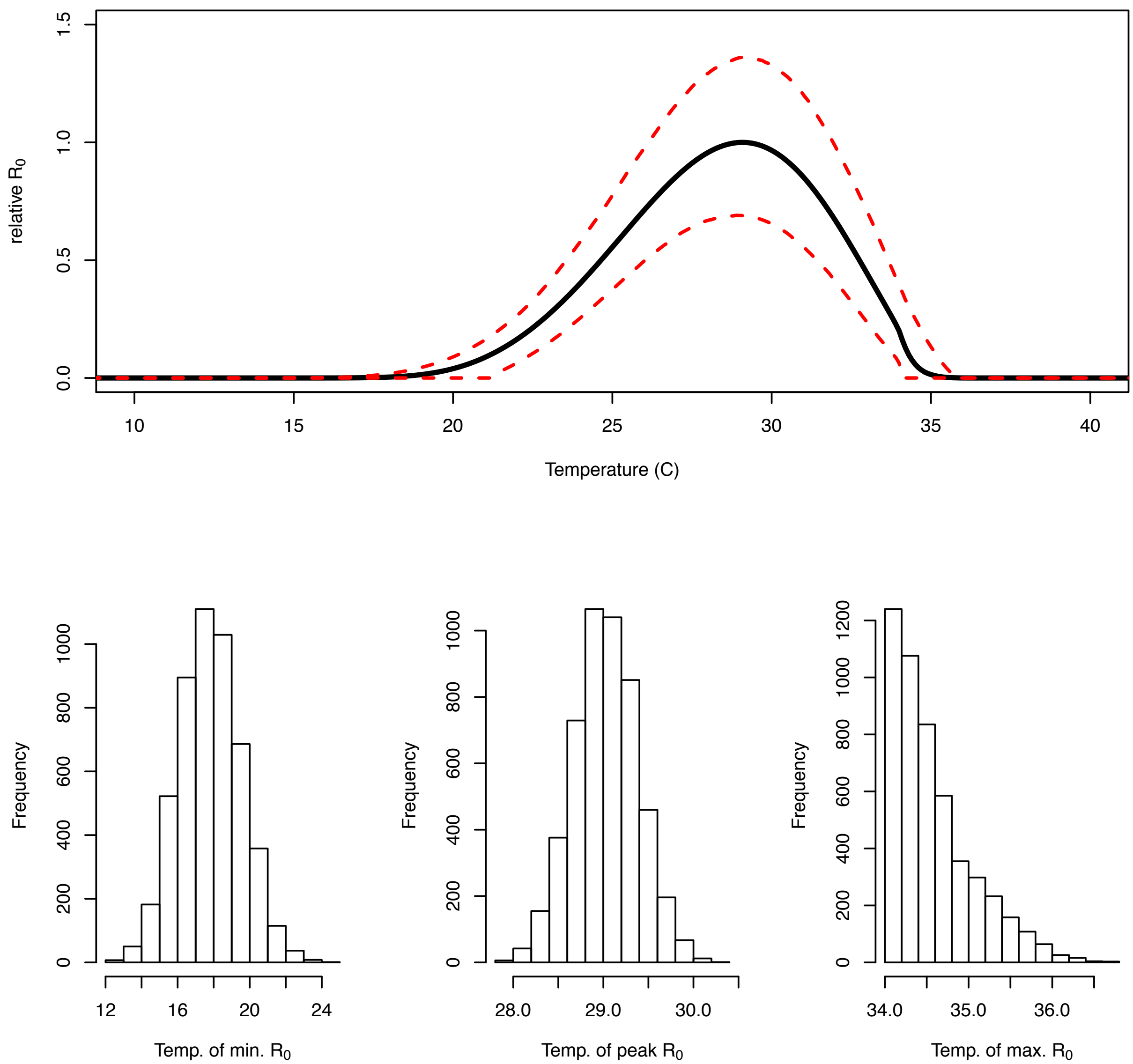

Fig. S5

Top, *Ae. aegypti* R_0 versus temperature, mean (black line) and 95% highest posterior density intervals (red dashed lines), for constant temperatures. Bottom, histograms of the minimum, maximum, and optimum temperatures for transmission.

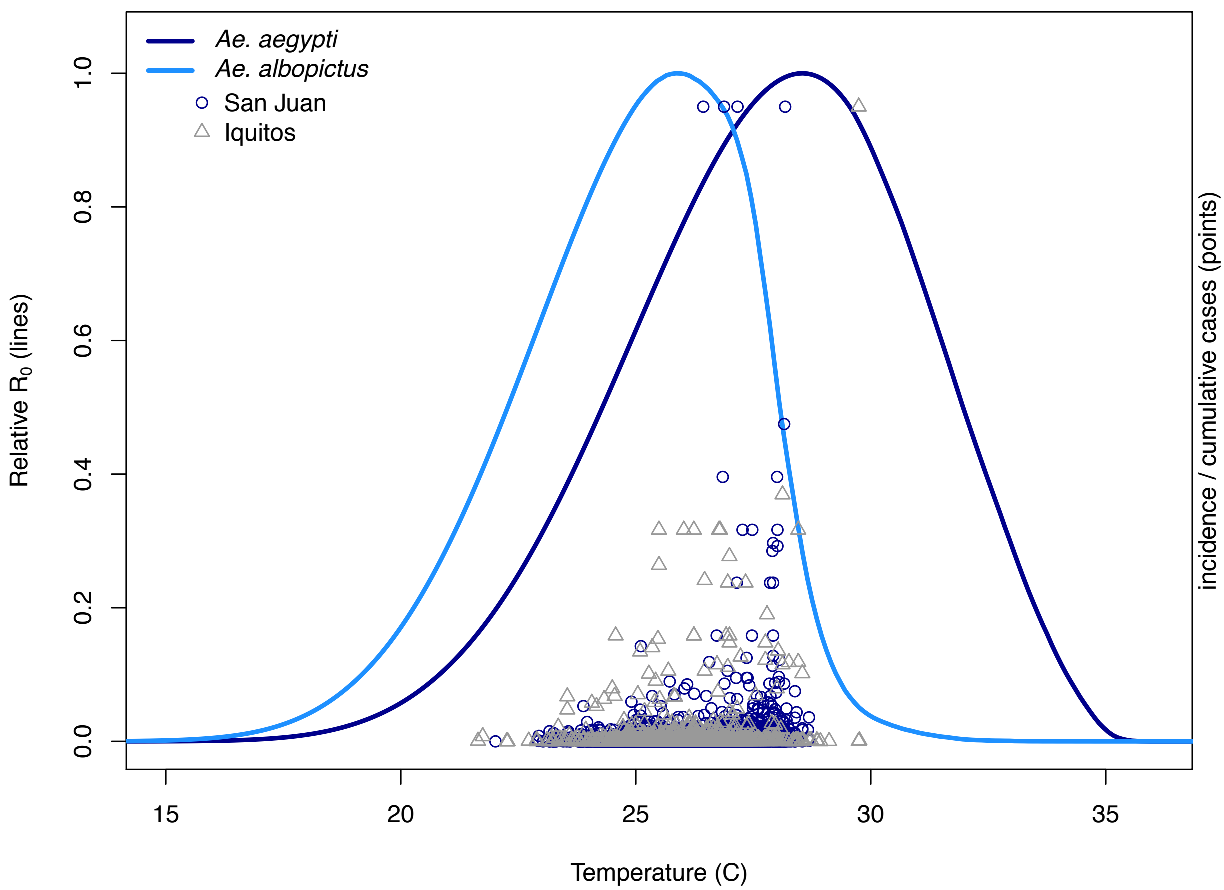

Fig. S6

Relative R_0 (assuming an 8°C daily temperature range) versus temperature for *Ae. aegypti* and *Ae. albopictus* (dark and light blue lines, respectively). For validation, weekly relative incidence of DENV (incidence divided by cumulative cases) in San Juan, Puerto Rico (blue circles) and Iquitos, Peru (gray triangles) are plotted against the mean temperature two weeks prior to each reporting date.

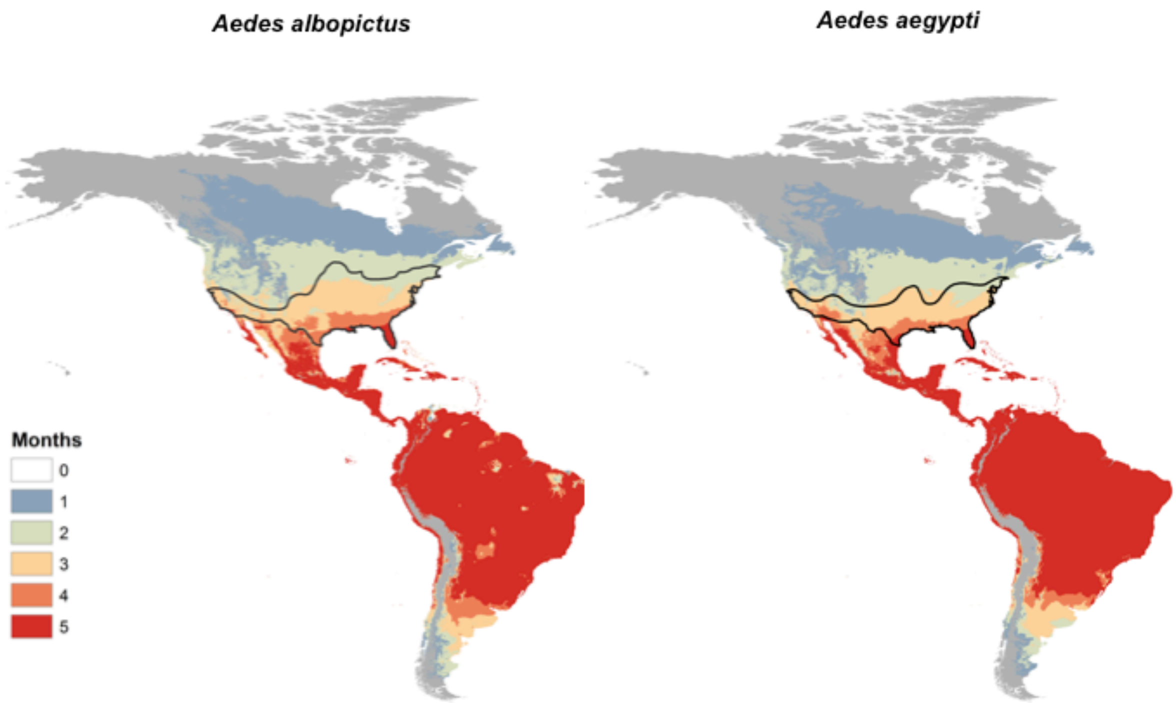

Fig. S7

Maps showing the number of months from August through the end of 2016 in which temperatures do not exclude transmission (Prob (R_0 > 0) > 0.5) by *Ae. albopictus* (left) and *Ae. aegypti* (right). Black lines indicate the current estimated range limits for the mosquito species in the United States, from the Centers for Disease Control and Prevention (CDC). This indicates the predicted temperature suitability for transmission following any cases exported from the Rio Olympics.

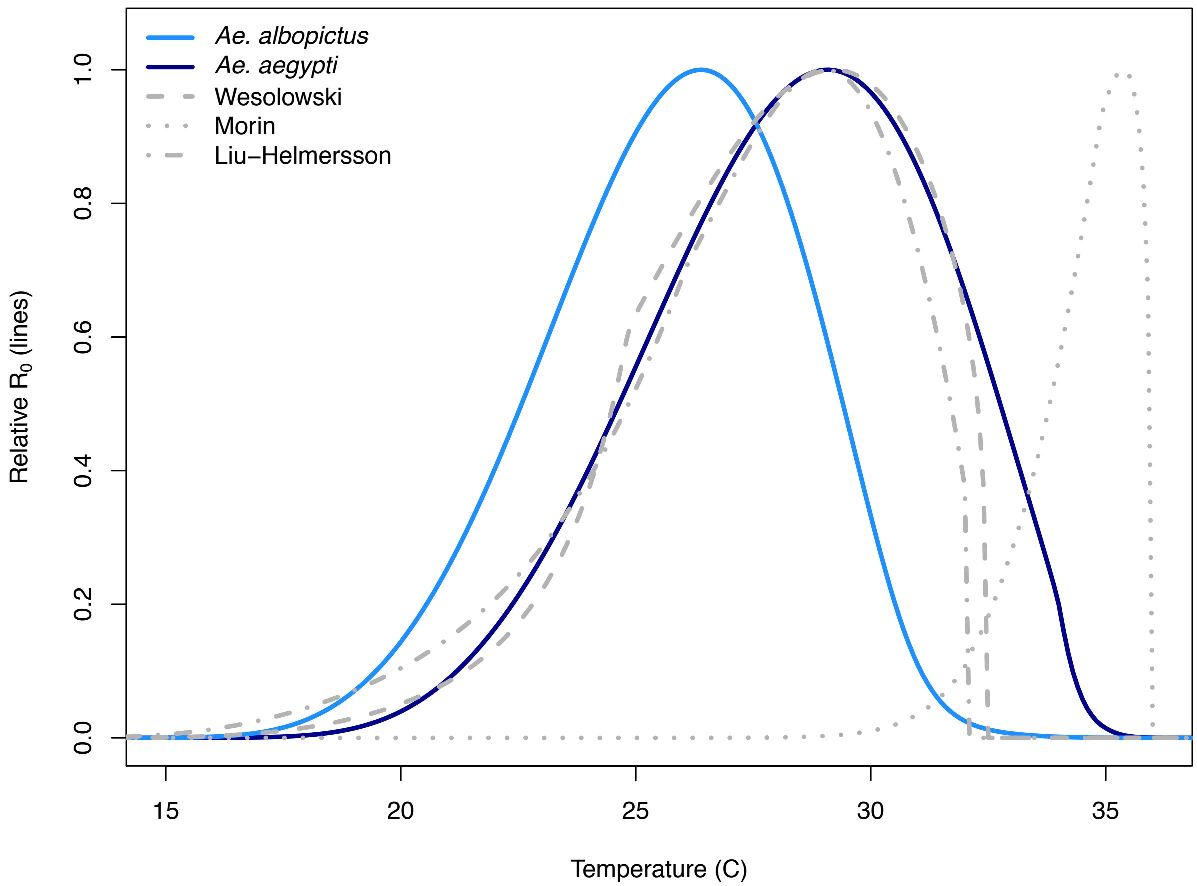

Fig. S8

R_0 versus temperature models for *Ae. aegypti* (dark blue line) and *Ae. albopictus* (light blue line) and models of DENV transmission by *Ae. aegypti* based on the thermal responses listed in three previous studies: Wesolowski et al. (1) (dashed gray line), Morin et al. (2) (dotted gray line), and Liu-Helmersson et al. (3) (dash-dotted gray line). We also attempted to plot the chikungunya $R_0(T)$ model from Johansson et al. (4) but could not reproduce their function (Fig. S1 therein) from the equations provided in the text.

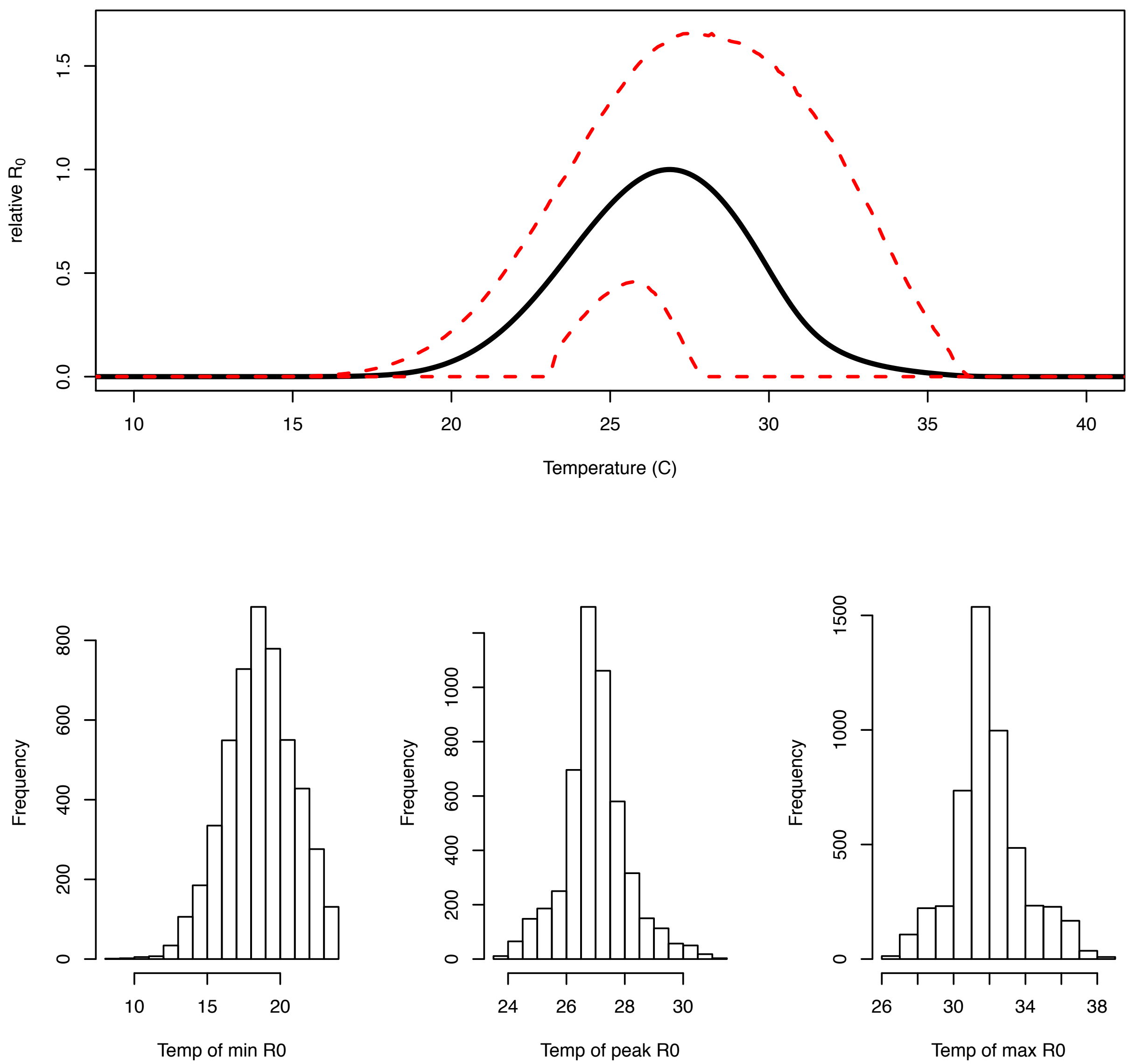

Fig. S9
Top, uninformative prior model of *Ae. albopictus* R_0 versus temperature model mean (black line) and 95% highest posterior density intervals (red dashed lines), for constant temperatures. Bottom, histograms of the minimum, maximum, and optimum temperatures for transmission.

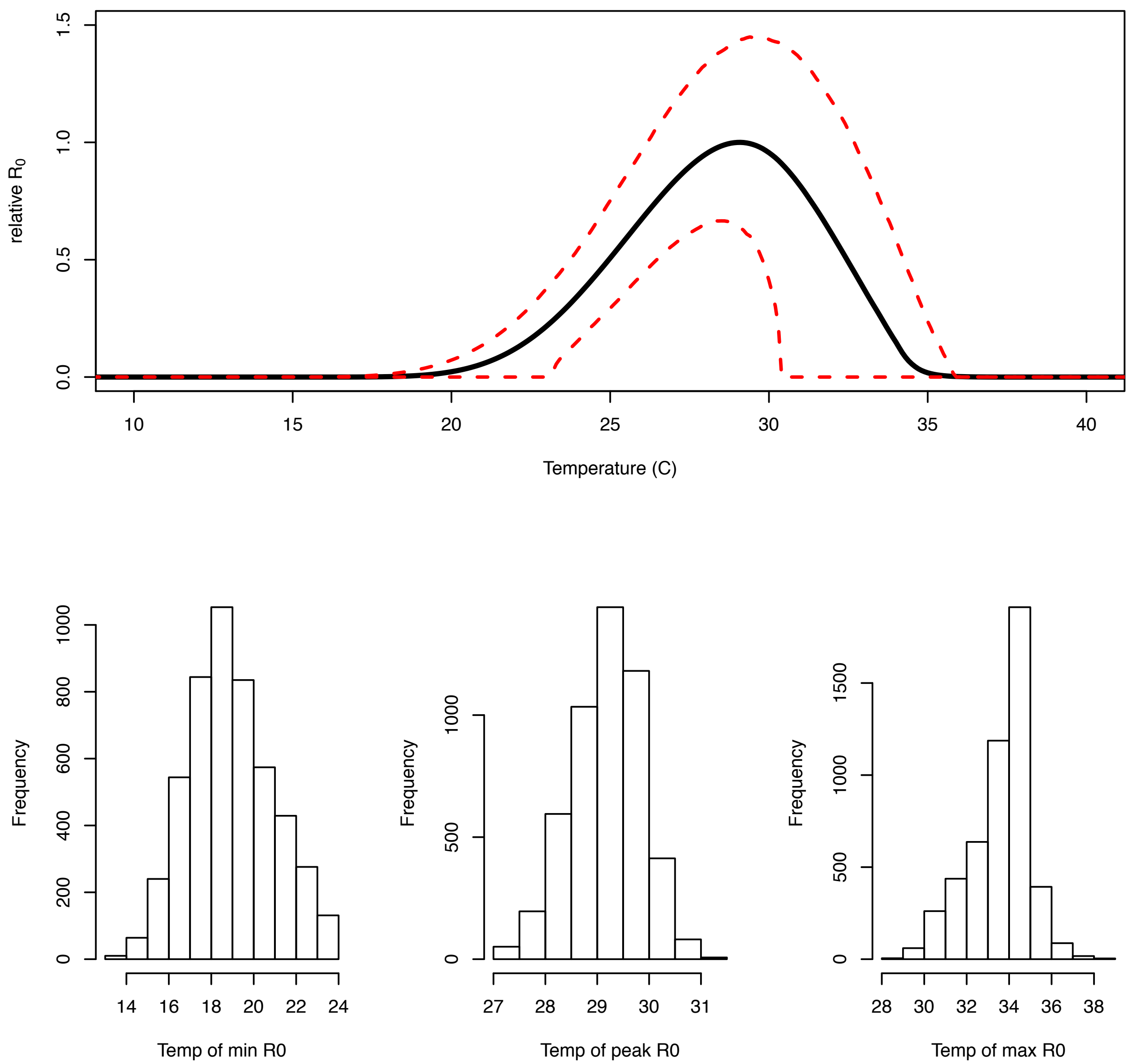

Fig. S10

Top, uninformative prior model of *Ae. aegypti* R_0 versus temperature model mean (black line) and 95% highest posterior density intervals (red dashed lines), for constant temperatures. Bottom, histograms of the minimum, maximum, and optimum temperatures for transmission.

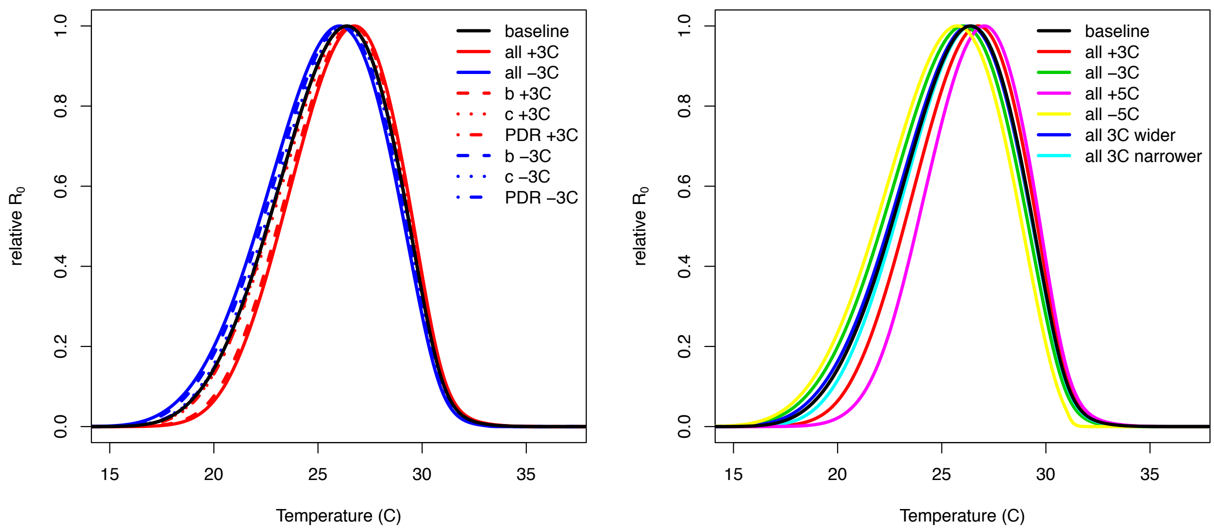

Fig. S11

Sensitivity analysis on the *Ae. albopictus* R_0 model at constant temperatures for vector competence (*b* and *c*) and parasite development rate (*PDR* = 1/extrinsic incubation period), in which these traits are shifted individually and together +/-3°C (left panel), or all three are shifted +/-3°C, +/-5°C, or the curves are made 3°C narrower or wider with the same optimum (right panel).

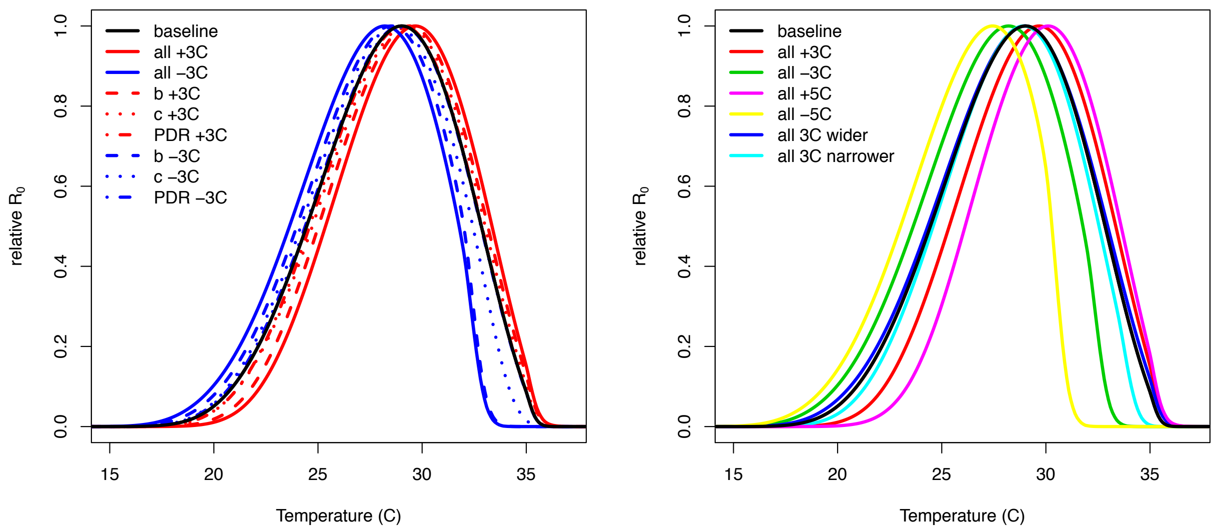

Fig. S12

Sensitivity analysis on the *Ae. aegypti* R_0 model at constant temperatures for vector competence (*b* and *c*) and parasite development rate (*PDR* = 1/extrinsic incubation period), in which these traits are shifted individually and together +/-3°C (left panel), or all three are shifted +/-3°C, +/-5°C, or the curves are made 3°C narrower or wider with the same optimum (right panel).

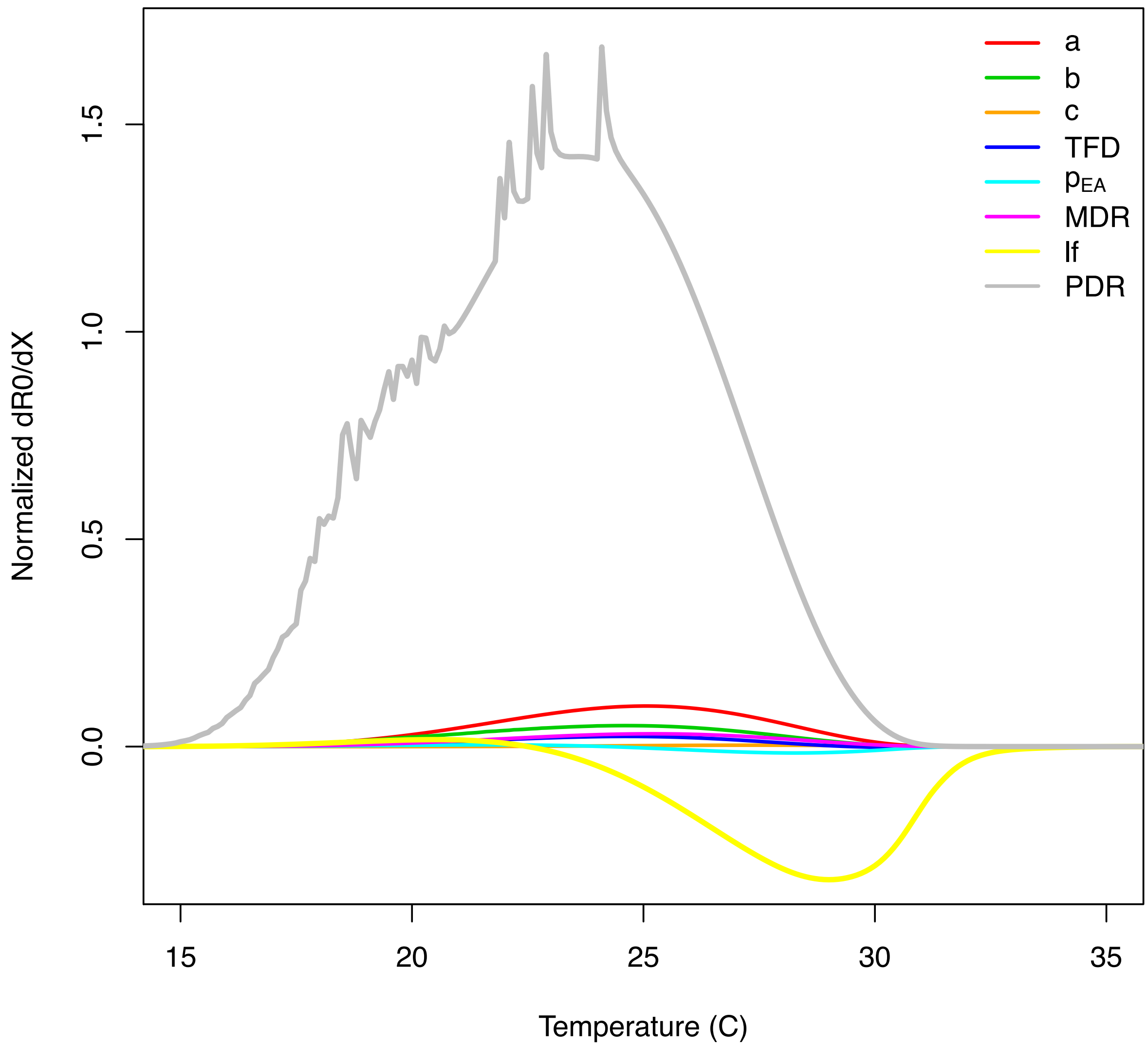

Fig. S13

Sensitivity analysis on the *Ae. albopictus* R_0 model, showing the derivative of R_0 with respect to each parameter, divided by R_0, at each temperature. Parasite development rate (PDR) has the largest effect on R_0 for most of the temperature range, while mosquito lifespan (lf) has a strong negative effect at warm temperatures. Parameter names are listed in Table 1.

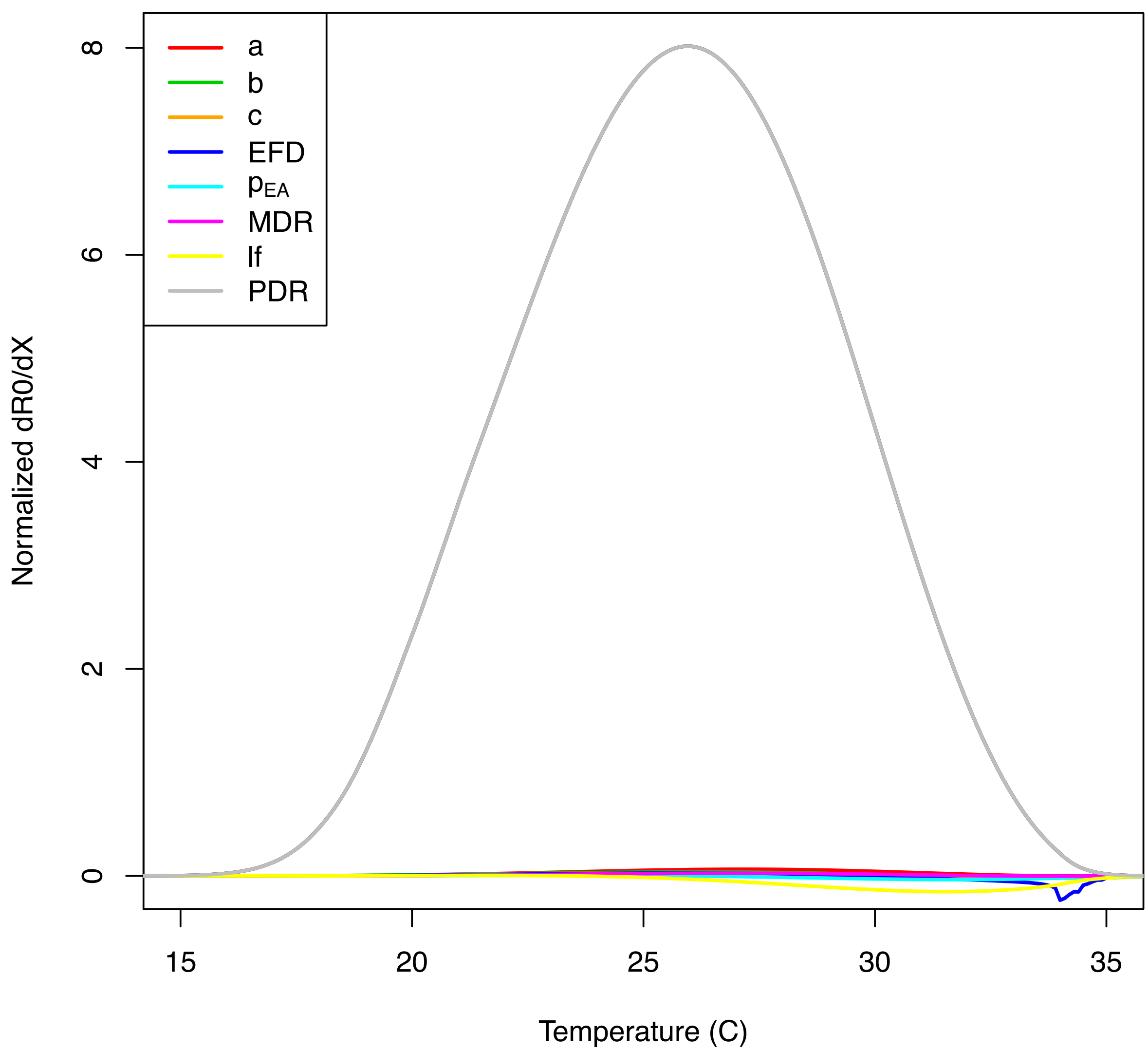

Fig. S14

Sensitivity analysis on the *Ae. aegypti* R_0 model, showing the derivative of R_0 with respect to each parameter, divided by R_0, at each temperature. Parasite development rate (PDR) has the largest effect on R_0 for most of the temperature range. Parameter names are listed in Table 1.

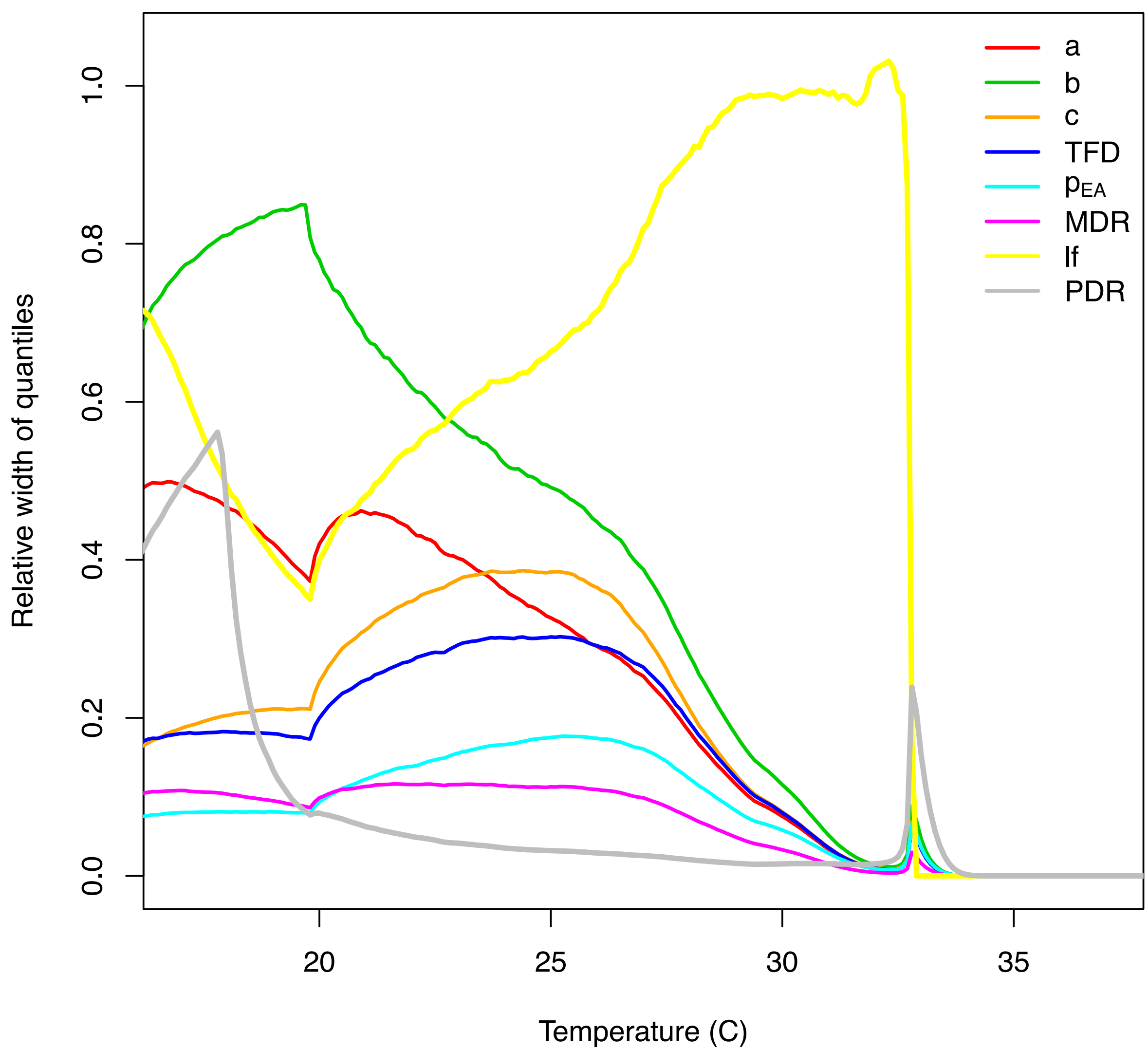

Fig. S15

Uncertainty analysis for *Ae. albopictus* R_0 model, showing the relative width of the 95% HPD intervals on R_0 that is due to each parameter, compared to the overall uncertainty. Each line shows the width of the 95% HPD interval on R_0 when calculated using draws from the posterior distribution of the focal parameter and the posterior means of the other parameters, divided by the width of the 95% HPD interval on R_0 when all parameters are drawn from their posterior distribution. This illustrates the degree to which uncertainty in R_0 arises from uncertainty in the component parameters at each temperature value. Mosquito infection probability (b) and lifespan (LF) dominate model uncertainty. Parameters are defined in Table 1.

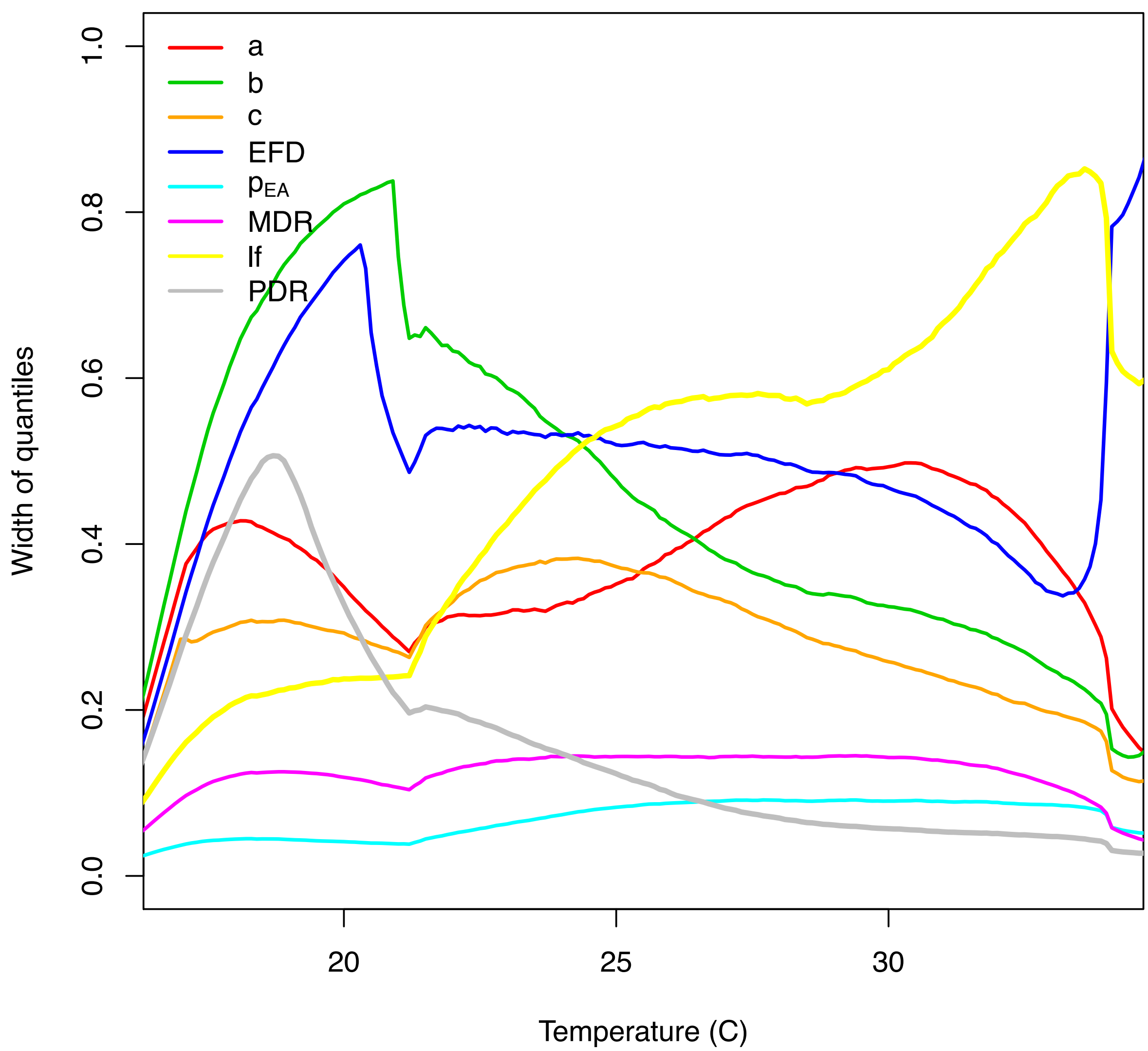

Fig. S16

Uncertainty analysis for *Ae. aegypti* R_0 model, as described in the caption for Fig. S14. Parameters are defined in Table 2.

Table S1.

Data used on the *Ae. albopictus* R_0 model. Each trait parameter symbol, definition, data sources, and thermal response function (Quad = quadratic) are shown on the left. Mean and 95% credible interval (95% HPD interval) for the critical thermal minimum (T_0), maximum, (T_m), and a rate constant (c) are given for each trait in the three right sections.

Trait	Definition	Refs	Function	T_0 Mean	T_0 95% CI		T_m Mean	T_m 95% CI		c Mean	c 95% CI	
a	biting rate, calculated as reciprocal of oviposition cycle length (1/days)	(5)	Brière	10.25	5.84	14.82	38.32	36.60	40.51	1.93E-04	1.27E-04	2.61E-04
TFD	eggs laid per female per gonotrophic cycle (number/female)	(5, 6)	Brière	8.02	3.18	13.08	35.65	35.00	36.51	4.88E-02	3.21E-02	6.72E-02
pEA	mosquito egg-to-adult survival probability	(5, 7–10)	Quad	9.04	6.37	11.67	39.33	37.17	41.62	-3.61E-03	-4.74E-03	-2.59E-03
MDR	mosquito egg-to-adult development rate (1/days)	(5–8, 10–14)*	Brière	8.60	4.43	12.29	39.66	37.78	41.70	6.38E-05	4.67E-05	8.23E-05
lf	mosquito adult lifespan (days)	(6, 11, 15)	Quad	13.41	10.53	16.11	31.51	29.14	33.57	-1.43E+00	-2.16E+00	-6.89E-01
b	probability that a mosquito infected with DENV becomes infectious (has virus in the salivary glands)	(16)	Brière	15.84	11.42	19.87	36.40	36.00	36.93	7.35E-04	4.36E-04	1.04E-03
c	probability that a mosquito fed on DENV-infected blood becomes infected	(16)	Brière	3.62	0.00	9.90	36.82	36.00	37.88	4.39E-04	3.29E-04	5.66E-04
PDR	DENV extrinsic incubation rate (reciprocal of the extrinsic incubation period: the time required	(16)	Brière	10.39	2.82	17.60	43.05	37.54	49.56	1.09E-04	5.45E-05	1.76E-04

for an exposed mosquito to become infectious; 1/days)			

Table S2.

Data used on the *Ae. aegypti* R_0 model. Each trait parameter symbol, definition, data sources, and thermal response function (Quad = quadratic) are shown on the left. Mean and 95% credible interval (95% HPD interval) for the critical thermal minimum (T_0), maximum, (T_m), and a rate constant (c) are given for each trait in the three right sections.

Trait	Definition	Refs	Function	T_0 Mean	T_0 95% CI		T_m Mean	T_m 95% CI		c Mean	c 95% CI	
a	biting rate, calculated as reciprocal of oviposition cycle length (1/days)	(2, 17)	Brière	13.35	8.27	17.41	40.08	40.00	40.28	2.02E-04	1.20E-04	2.80E-04
EFD	eggs laid per female per day (number/female/day)	(18, 19)	Brière	14.58	8.08	20.60	34.61	34.00	35.77	8.56E-03	3.78E-03	1.41E-02
pEA	mosquito egg-to-adult survival probability	(7, 20–23)	Quad	13.56	12.56	14.51	38.29	37.54	39.02	-5.99E-03	-6.82E-03	-5.13E-03
MDR	mosquito egg-to-adult development rate (1/days)	(7, 20–24)	Brière	11.36	7.19	15.03	39.17	39.00	39.54	7.86E-05	5.75E-05	9.93E-05
lf	mosquito adult lifespan (days)	(18, 19)	Quad	9.16	6.69	12.33	37.73	35.68	39.89	-1.48E-01	-2.06E-01	-9.77E-02
b	probability that a mosquito infected with DENV becomes infectious (has virus in the salivary glands)	(25–27)	Brière	17.05	12.56	21.26	35.83	35.06	36.69	8.49E-04	5.07E-04	1.20E-03
c	probability that a mosquito fed on DENV-infected blood becomes infected	(25, 27)	Brière	12.22	5.61	17.76	37.46	35.70	39.29	4.91E-04	3.33E-04	6.41E-04
PDR	DENV extrinsic incubation rate (reciprocal of the extrinsic incubation period: the time required for an exposed mosquito to become infectious; 1/days)	(25, 27–31)	Brière	10.68	3.86	18.33	45.90	39.73	52.92	6.65E-05	3.60E-05	1.09E-04

Table S3.

Aedes spp. trait thermal response data used to generate informative priors for the main *Ae. albopictus* and *Ae. aegypti* R_0 models. Mean and 95% credible interval (95% HPD interval) for the critical thermal minimum (T_0), maximum, (T_m), and a rate constant (c) are given for each trait in the three right sections.

Trait	Definition	Refs	Function	T_0			T_m			c		
				Mean	95% CI		Mean	95% CI		Mean	95% CI	
a	biting rate, calculated as reciprocal of oviposition cycle length (1/days)	(15)	Brière	14.67	10.67	18.34	41.00	37.56	44.99	2.71E-04	1.59E-04	4.09E-04
EFD	eggs laid per female per day (number/female/day)	(32)	Brière	14.06	11.32	16.60	32.03	30.95	33.35	2.08E-02	1.36E-02	2.89E-02
pEA	mosquito egg-to-adult survival probability	(33)	Quad	7.68	6.48	8.90	38.31	36.99	39.57	-3.36E-03	-4.02E-03	-2.72E-03
MDR	mosquito egg-to-adult development rate (1/days)	(32, 33)	Brière	15.12	9.56	19.93	37.67	36.54	38.45	1.49E-04	8.59E-05	2.17E-04
lf	mosquito adult lifespan (days)	(32)	Quad	16.63	15.93	17.25	31.85	31.16	32.64	-1.24E+00	-1.50E+00	-9.76E-01
b	probability that a mosquito infected with flavivirus becomes infectious (has virus in the salivary glands)	(34)	Brière	12.05	8.18	15.09	32.79	32.02	34.32	9.86E-04	5.97E-04	1.34E-03
c	probability that a mosquito fed on flavivirus-infected blood becomes infected	(34)	Brière	1.51	0.00	4.11	34.74	32.87	37.18	5.23E-04	4.10E-04	6.32E-04
PDR	WNV, SLEV, WEEV extrinsic incubation rate (reciprocal of the extrinsic incubation period: the time required for an exposed mosquito to become infectious; 1/days)	(35)	Brière	11.50	3.43	18.55	38.97	33.08	45.00	1.04E-04	3.79E-05	1.93E-04